Characterisation at infra-red wavelengths of metamaterials formed by thin-film metallic split-ring resonator arrays on silicon

Nigel P. Johnson[1], Ali Z. Khokhar[1], Harold M. H. Chong[1], Richard M. De La Rue[1] and Scott McMeekin[2]

The infra-red reflectance spectra at normal incidence for split ring resonator (SRR) arrays fabricated in thin films of three different metals on a silicon substrate are reported. The results are compared with a finite difference time domain (FDTD) simulation of the structures and a simple and novel equivalent-circuit method for the calculation of the first and second resonant wavelengths.

Introduction: Metamaterials [1] have received much attention due to their potential for exploiting negative ε and negative μ, which can give rise to negative refraction [2] and perfect lensing [3]. Metamaterials have arrays of elements that have a typical size that is one tenth the wavelength of the light with which they interact. Typical elements are Split Ring Resonators (SRRs), which are sensitive to the polarisation of the incident radiation. For a truly negative refractive index (or 'left-handed') material it is necessary to have both negative μ and negative ε simultaneously over a particular frequency range. For simple planar arrays of split ring resonators this condition only occurs for in-plane incident geometries [4,5]. However, for light incident normally on to the SRRs and either TE or TM polarisation, remarkable differences in the transmission and reflection spectra are obtained [6]. Similarly, by opening and closing the rings, substantial changes

can be obtained in the reflection (and transmission) spectra. So far this behaviour has only been achieved by separate fabrication of open and closed SRRs, but a similar effect can be obtained by rotating the polarisation of the incident light. Most of the meta-materials described in the literature to date are passive structures. To obtain increased functionality it is desirable to be able to change the properties of one or more of the individual elements in the array. Steps towards increasing functionality include the use of a potentially active substrate such as silicon, while it is also of interest to study the influence of alternative choices of the metal used in constructing the elements.

Experimental: We have investigated the use of three different metals to form the SRRs, as the basis for future fabrication of active metamaterial arrays on a potentially active material, i.e. silicon. Gold SRRs have been fabricated previously on silica [5] - and in this letter we compare the results obtained for gold, aluminium and silver structures on silicon. Gold is traditionally avoided in a silicon VLSI foundry because of its ability to form deep levels in the silicon. Aluminium is the most commonly chosen metal in silicon VLSI - and has a higher bulk plasma frequency than silver or gold.

Typical experimental and computed reflectance spectra are shown in Fig. 1. In TE polarisation, with the electric field oriented across the SRR gaps, two reflectance peaks are observed for the particular structure being measured: one sharper resonance occurs at around a 3 µm wavelength, while a broader peak is

observable at around 8 μm. A micrograph representative of the samples is shown in Figure 2.

Theory: The longer wavelength peak is dependent upon what can be considered as essentially the LC electrical resonance of a metal SRR - and is given by the equation [5] $\omega_{LC}=(L_T C_T)^{-1/2}$ where L_T is the total inductance formed by the combination of the self inductance of the rectangular loop forming the SRR element, L_{Ring}, and the mutual inductance formed between the conducting arms of neighbouring SRR elements, L_{mut}. An expression for the self-inductance of a complete rectangular loop made from rectangular cross-section wire is given by [7]:

$$L_{Ring} = 0.2\mu_o \left(-\frac{w}{2}\sinh^{-1}1 + \frac{w}{2}\sqrt{2} + \left(l - \frac{w}{2}\right)\sinh^{-1}\left(\frac{l - \frac{w}{2}}{w/2}\right) - \sqrt{\left(l - \frac{w}{2}\right)^2 + \left(\frac{w}{2}\right)^2} \right) \quad H.....(1)$$

- while the mutual inductance of two parallel rectangular conductors is given by [8]:

$$L_{Mutual} = 0.2.l\left(\ln\left(\frac{l}{d} + \sqrt{1 + \frac{l^2}{d^2}}\right) - \sqrt{1 + \frac{d^2}{l^2}} + \frac{d}{l} \right) \quad \mu H..............(2)$$

where, referring to Fig. 3, l is the length of the SRR element, w is the width of the wire forming the split ring, t is the thickness of the wire - and d is the centre-to-centre separation between the arms of adjacent SRR elements.

Previously only the parallel plate capacitance of the gap in the SRR element has been taken into account when considering the capacitance of the SRR array [5].

However, in order to calculate the total capacitance of the SRR element, C_T, it is necessary to take into account the parallel plate and co-planar capacitances formed between both the individual SRR elements, C_e, and the capacitance formed by the gap in the SRR structure, C_g. The parallel plate capacitance of both components can be calculated from the standard equation $C = \varepsilon_o \varepsilon_r$(area/separation), while the co-planar capacitance can be calculated by using conformal mapping techniques to take into account the field that is present in the substrate. The general form of the equation for the co-planar capacitance per unit length for two metal strips of width p, separated by distance q, is given by [9]:

$$C_{cp} = \frac{(\varepsilon_r + 1)\varepsilon_o}{2} \frac{1}{\pi} \ln\left[2\frac{1+\sqrt{k'}}{1-\sqrt{k'}}\right] \quad F/m \ldots\ldots(3)$$

where k' is a geometrical factor given by:

$$k' = \sqrt{\left(1-\left(\frac{p}{p+2q}\right)^2\right)} \ldots\ldots\ldots\ldots(4)$$

The shorter wavelength peak in the reflectance spectrum shown in Fig. 1 can be identified as the reduced plasma frequency [10] and is a collective property of the SRR array. This resonance has relatively low dependence on shape and, at frequencies in the infra-red part of the spectrum, is also not strongly dependent on the particular metal used. The resonant frequency of the peak is dependent upon the dilution of the metal and is inversely proportional to the natural logarithm of the filling fraction given by the ratio of the period of the SRR array to the radius of extended cylindrical pillars [10]. To take into account the more

complex geometry of the SRR elements - and the fact that they are closely packed - a factor F is introduced, which is the area of exposed silicon in a unit cell, i.e the total area of the unit cell minus the area covered by the metallic SRR.

A modified expression for the reduced plasma frequency may then be written as:

$$\omega_p^2 = \frac{c^2.2\pi}{a^2.\ln\left(a^2/F\right)n_{eff}^2} \qquad \text{rad s}^{-1} ....(5)$$

where n_{eff} is the effective refractive index of the dielectric medium at the frequency of the infra-red radiation interacting with the SRR array. The value of n_{eff} is approximately 70% of the value of silicon and is related to the distribution between silicon and air of the electric flux density interacting with the SRR array. As the metal area of an individual SRR increases, for a fixed unit cell area, F decreases - and the plasma frequency also decreases. This effect is greatest at the smallest spacing between SRRs, where the position of the peak diverges substantially from the simple theory.

Results: In Table 1 the experimental values of the shorter wavelength resonant peak, of the reduced plasma frequency and of the longer wavelength LC resonant peak are compared with the values calculated using finite difference time domain (FDTD) simulations and the values calculated using the equivalent circuit analysis presented above. Agreement is typically within 10 %, but diverges for smaller separation between elements to 20%. In general, the peak resonant wavelengths for the experimental results are at shorter wavelengths than either simulations or the models. Over the experiment results, simulations and

equivalent circuit analysis there is little effect produced by changing the metal at these wavelengths. Other features to note are the line-width of the plasmon resonance (the shorter wavelength peaks) in the two orthogonal polarisations. The peak is wider by around a factor of two for TM excitation in comparison with TE polarisation.

In conclusion: we have fabricated and measured SRR arrays on silicon realised in three different metals. The positions of the peaks can be closely modelled by FDTD simulations and by relatively simple electric and magnetic modelling. The plasmon resonance is given by a modified [Drude] model that takes into account the spacing between SRRs and not simply the area dilution factor. The model for the LC resonance can be refined using the expression for the self and mutual inductances of an SRR element and coplanar capacitance - in parallel with the SRR gap capacitance for individual elements and the effective capacitance between neighbouring elements. There is little difference between the EM properties of the different metals at the infra-red wavelengths considered.

References

1   Veselago V G 1967 Usp. Fiz Nauk 92 517 or Veselago V G 1968 Sov. Phys – Usp 10 509. (English Translation)
2   M. Notomi, "Negative refraction in photonic crystals." Optical and Quantum Electronics 34: 133–143, 2002.
3   J. B. Pendry "Negative Refraction Makes a Perfect Lens." Phys. Rev. Lett., 85, 3966 (2000).
4   George Goussetis, Alexandros P Feresidis, ShenhongWang,Yunchuan Guo and John C Vardaxoglou, "Uniplanar left-handed artificial metamaterials." J. Opt. A: Pure Appl. Opt. 7 (2005) S44–S50

5   S Linden, C Enrich, M Wegener,Ji Zhou, Thomas K, C M. Soukoulis "Magnetic response of metamaterials at 100 Terahertz." Science 306, 1351 (2004).

6   Nigel P Johnson, Ali Z Khokhar, Harold M Chong, Chongjun Jin, Jharna Mandel, Scott McMeekin and R M De La Rue, "Increasing Optical Metamaterials Functionality." Proc. SPIE 5955 59550O-1-59550O-6 (2005). Metamaterials Ed Tomasz Szoplik, Ekmel Ozbay, Costas M Soukoulis, Nikolay I Zheludev

7   Zahn M, "Electromagnetic Field Theory" pp343, John Wiley & Sons, 1979.

8   Grover F. W. "Inductance Calculations, Working Formulas and Tables", pp 35 Dover Pub. 1946.

9   Wheeler H. A. "Transmission-line properties of parallel strips separated by a dielectric sheet." IEEE Trans Microwave Theory Tech. MTT-13, 1965, pp172-185.

10   J B Pendry, A J Holden, D J Robbins and W J Stewart, "Low frequency plasmons in thin-wire structures." pp4785- 4809 J. Phys.: Condens. Matter 10 (1998).

Author's affiliations:

1. Nigel P. Johnson, Ali Z. Khokhar, Harold M. H. Chong, and Richard M. De La Rue (Department of Electrical and Electronic Engineering, University of Glasgow, Oakfield Avenue, Glasgow, G12 8QQ, United Kingdom)

2. Scott McMeekin (Department of Electrical and Electronic Engineering, School of Science Engineering and Design, Glasgow Caledonian University, Cowcaddens Road, Glasgow, G4 0BA, United Kingdom)

Figure 1. Reflectance spectra for aluminium sample showing: (a) experimental and (b) simulated TE and TM resonant peaks.

Figure 2. Micrograph of the silver SRR sample detailed in Table 1.

Figure 3. Two elements of an SRR array that is infinite in both in-plane dimensions.

Table 1. Comparison of peak resonant wavelengths for SRR of various metals from experimental measurement, FDTD simulation and calculated from the plasma frequency and LC resonance. The metal thickness for all samples is nominally 30 nm.
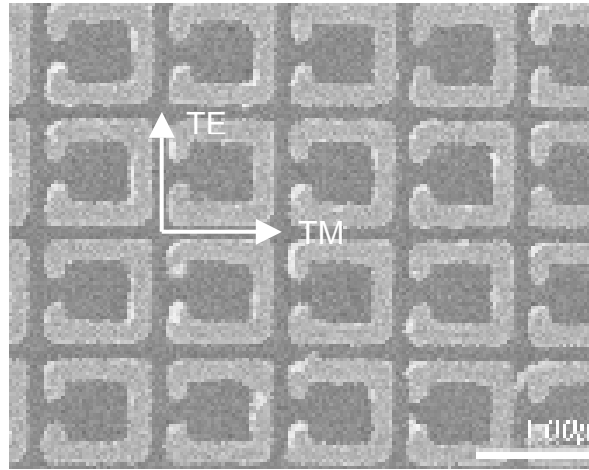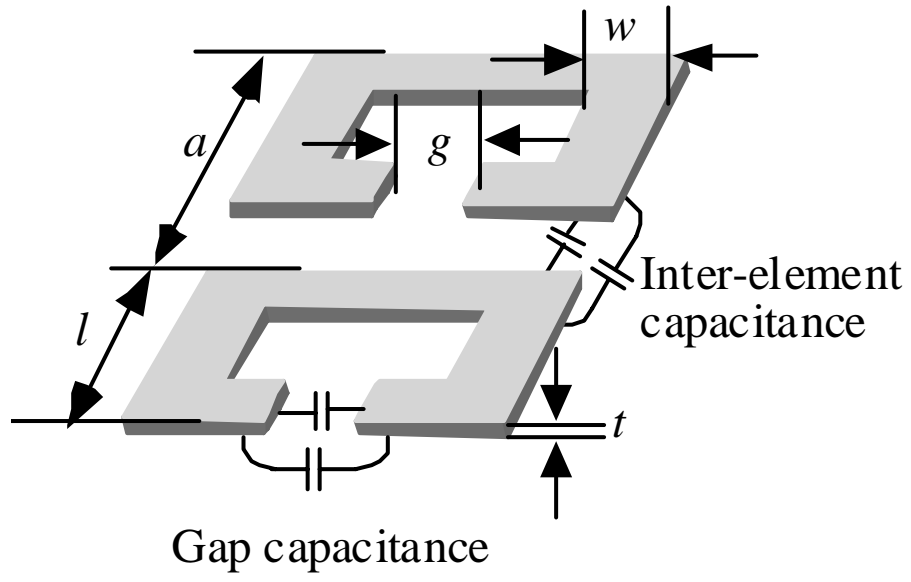
Figure 1.

(a)

(b)

Figure 2.

Figure 3.

Gap capacitance

Inter-element capacitance
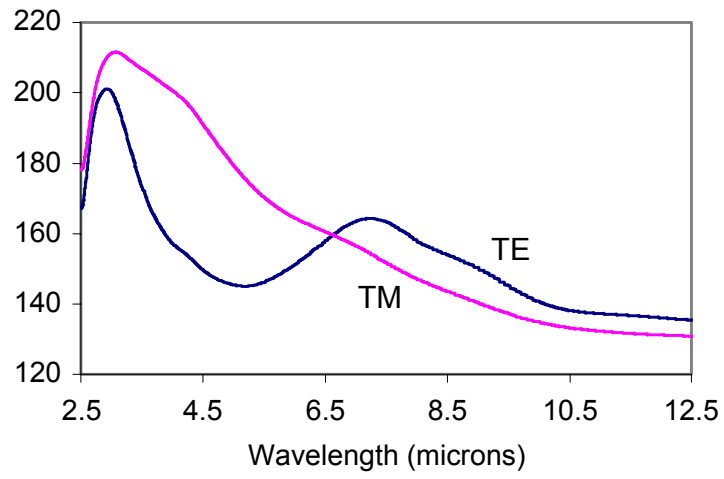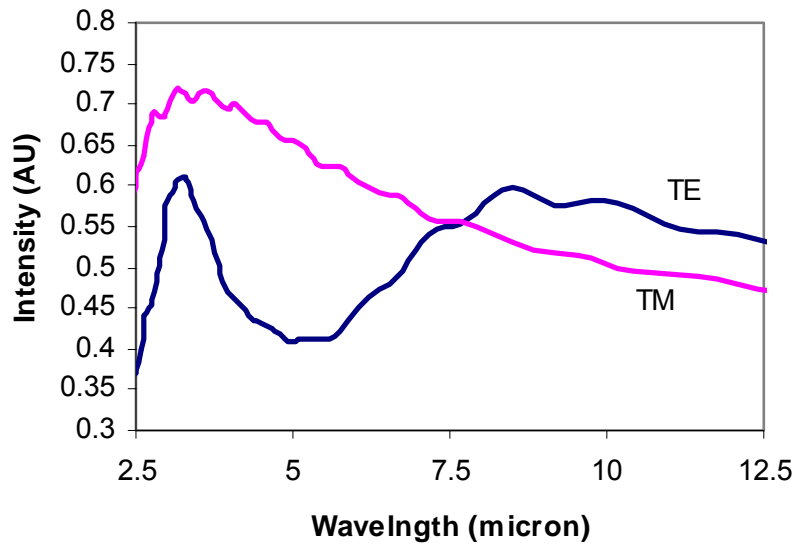
Table 1.

Sample					λ_{TE1} (micrometres)			λ_{TE2} (micrometres)		
Metal	l	a	w	g	Exp	FDTD	Plasma	Exp	FDTD	LC
Ag-1	572	667	110	120	3.02	3.1	3.4	8.2	8.5	8.4
Al-1	564	616	120	130	2.95	3.1	3.6	8.2	8.6	8.6
Al-2	564	664	110	130	2.95	3.1	3.3	8.1	8.5	8.9
Au-1	552	614	90	22	3.54	4.2	3.2	10.0	12.5	10.5
Au-2	217	297	66	33	1.35	1.7	1.5	3.1	4.3	2.5